GLIA 3:81–97 (1990)

Immunohistochemical Localization of Glutamine Synthetase in Mesencephalon and Telencephalon of the Lizard *Gallotia galloti* During Ontogeny

M. MONZON-MAYOR,[1] C. YANES,[2] G. THOLEY,[3] J. DE BARRY,[4] AND G. GOMBOS[4]
[1]*Departamento de Histologia, Colegio Universitario de Las Palmas (Division de Medicina), Universidad de Las Palmas de G.C.;* [2]*Departamento de Biologia Celular, Facultad de Biologia, Universidad de La Laguna, Tenerife, Canary Islands, Spain;* [3]*Laboratoire de Microbiologie, Université Louis Pasteur;* [4] *Centre de Neurochimie du C.N.R.S. and U 44 INSERM, 67000 Strasbourg, France*

KEY WORDS Radial glia, Phylogenesis, Astrocytes, Immunohistochemistry, Intermediate filaments, Reptile

ABSTRACT The immunohistochemical localization of glutamine synthetase, an astrocyte marker in mammals, was determined in the telencephalon and mesencephalon of the lizard *Gallotia galloti* during development by using an antiserum raised against chicken brain glutamine synthetase. Ependymal glial cells and their radial processes were glutamine synthetase immunoreactive, and they were present also in the adult. Immunoreactivity was also detected in two populations of scattered cell bodies, each preferentially localized in different zones: star-shaped cells morphologically similar to mammalian astrocytes, and ovoid or pear-shaped cell bodies, the processes of which were aligned with radial fibers and formed perivascular end-feet. Both populations displayed ultrastructural characteristics of astrocytes even though a comparison with our previous results (Monzon-Mayor et al., 1989; Yanes et al., 1989) indicated that many of these cells did not react with antibodies directed against the astrocyte-specific glial fibrillary acidic protein.

During ontogeny, glutamine synthetase immunoreactivity appeared in radial glial processes and in ependymal glial cells of midbrain at embryonic stage 35 (E35) and of telencephalon at E37; in both regions, immunoreactivity in the radial glia increased until hatching and then decreased until adulthood, but it did not disappear. Labelled scattered cells became progressively more numerous and more immunoreactive.

A comparative analysis of the distribution of these cells at different ages tends to suggest that some of the "ovoid" astrocytes originate in, and migrate out from, the proliferative zone of the different sulci, whereas the star-shaped cells appear directly in situ, probably because they begin to express glutamine synthetase after they have reached their final location.

INTRODUCTION

Glutamine synthetase (GS, EC:6.2.1.2.) is the enzyme that catalyzes the formation of glutamine from glutamate and ammonia; it is thus involved in different cellular mechanisms such as ammonia detoxication (Weil-Malherbe, 1962) and supply of the glutamine amino group for the synthesis of purine and pyrimidine bases. In the nervous system, glutamine is involved in the synthesis of the neurotransmitter glutamate (Hamberger et al., 1979).

Received February 15, 1989; accepted September 25, 1989.

Abbreviations used: A, Astrocyte; ADVR, anterior dorsal ventricular ridge; Amc, nucleus centralis amygdalae; Ame, nucleus externus amygdalae; bv, blood vessel; ca, commissura anterior; CNS, central nervous system; DC, dorsal cortex; DMC, dorsomedial cortex; EC, endothelial cells; ef, end-feet or -foot; FLM, fasciculus longitudinalis medialis; Ic, n. isthmi, pars magnocellular caudalis; Ip, n. interpeduncularis; Ir, n. isthmi, pars magnocellularis rostralis; Isp, n. isthmi, pars parvocellularis; LC, lateral cortex; mc, migrating (?) cells; MC, medial cortex; N, neurons; Nsa, nucleus septalis anterior; Nsd, nucleus septalis dorsalis; Nsl, nucleus septalis lateralis; NTOL, nucleus tracti olfactorii lateralis; nIII, n. oculomotorius; nIV, n. trochlearis; nV, n. nervi trigemini; och, optic chiasma; opt, n. opticus tegmenti; ot, optic tract; OT, optic tectum or tectum mesencephali; pm, pia mater; Pr, n. profundus mesencephali; PT, pretectal zone; RF, radial fibers; rub, n. ruber; SA, silvius aqueduct; sl, sulcus lateralis; slH, sulcus limitans of his; st, sulcus terminalis; StV, striatum ventralis; sv, sulcus ventralis; TS, torus semicircularis; TZ, tegmental zone; V, ventricle.

Address reprint requests to Dr. M. Monzon-Mayor, Departamento de Histologia, Colegio Universitario de Las Palmas (Division de Medicina), Universidad de Las Palmas de G. C., Canary Islands, Spain 316022.

Immunocytological studies show that, in adult mammals, glutamine synthetase is present in both protoplasmic and fibrous astrocytes and in their subpial and perivascular processes, in subependymal structures, and in retinal Müller cells, whereas neurons, oligodendrocytes, pericytes, and endothelial cells are glutamine synthetase negative (Caldani et al., 1982; Didier et al., 1986; Martinez-Hernandez et al., 1977; Norenberg, 1979, 1983; Norenberg and Martinez-Hernandez, 1979; Riepe and Norenberg, 1977). Glutamine synthetase is also present in mammalian astrocytes cultured in vitro (Hallermayer et al., 1981; Hallermayer and Hamprecht, 1984; Patel and Hunt, 1985; Patel et al., 1985; Patel, 1986; Schousboe et al., 1977): its activity increases with astrocyte maturation, and it is induced by glucocorticoids (Juurlink et al., 1981; Moscona and Piddington, 1966; Patel et al., 1983a,b, 1986; Tardy et al., 1984; Tholey et al., 1985). In the chick brain, GS cellular localization, studied with antichick brain GS antibodies, appeared to be the same as in mammals (Tholey et al., 1987a,b). This indicates a phylogenetically stable cellular localization of GS. This is true, however, only in the tissue, as cultured chicken neurons are immunoreactive (Tholey et al., 1987a,b).

Glial fibrillary acidic protein (GFAP) is usually used as marker for astrocytes and ependymal glial cells, which often also contain GS. Tanicytes are GS-negative (Norenberg and Martinez-Hernandez, 1979; Didier et al., 1986), although GFAP-positive (Bignami and Dahl, 1974; Dahl et al., 1985; Ludwin et al., 1976; Norenberg and Martinez-Hernandez, 1979; Didier et al., 1986). We have previously used anti-GFAP and antivimentin antibodies to study glial cell distribution during development of *Gallotia galloti* CNS (Monzon et al., 1989; Yanes et al., 1989). We showed that in this lizard GFAP-positive radial glia is still present in the adult, together with scattered GFAP-positive cells. Sometimes the aspect of these cell bodies was not star-shaped, but round or pear-shaped; their GFAP-immunoreactivity, however, designates them as astrocytes. At early embryonic ages, these cells are GFAP-negative but vimentin-positive; during development a shift from vimentin- to GFAP-positivity occurs, although some radial fibers and end-feet remained vimentin-positive even in the adult.

The present report provides data, not available in the literature, on glutamine synthetase localization in reptile CNS and complements our previous studies on gliogenesis in *Gallotia galloti*.

MATERIALS AND METHODS

Antibodies

The antichick glutamine synthetase immunoserum used was raised in rabbits and was described and characterized by Bloch et al. (1984) and Sena et al. (1988). The secondary antibodies were sheep antirabbit Ig conjugated with either fluoresceine isothiocyanate (FITC) or horseradish peroxidase (HRP), purchased from Pasteur Production (Paris, France).

Animals and Tissue Fixation

We used a total of 50 embryos (from E-32 to hatching), 50 young animals (from the 5th to the 15th postnatal day) and 60 adults of *Gallotia galloti* (Bischoff, 1982) (family Lacertidae; order Squamata), a lizard indigenous to the island of Tenerife. The stages of the embryo development were defined according to the tables of equivalence between the development of the *Gallotia galloti* (Ramos, 1980) and of *Lacerta vivipara* (Dufaure and Hubert, 1961).

Embryonic and very young lizards were decapitated and their heads immersed for about 2 days in the fixative (2% paraformaldehyde and 0.25% glutaraldehyde in PBS:0.15 M NaCl in 0.1 M phosphate buffer, pH 7.2); the CNS of adults was fixed in situ by intracardiac perfusion with the same fixative. The skull then was opened, and the telencephalon and brainstem were excised, cleaned from meninges, and then immersed for 3 to 4 hours in the fixative.

Handling of the embryo sections was very difficult due to their small size; thus, the encephalon and brainstem of embryos and young animals were embedded in 4% agarose before slicing into 50 to 100 μm sections with a Vibratome (Oxford instrument, Foster City). Sections were kept at +4°C until processed as described below.

Immunohistochemistry

All incubations were performed at room temperature unless otherwise specified. Antibodies were diluted in PBS for immunofluorescence and immunoperoxidase techniques, and after each step the sections were washed three times (for 10–15 minutes each time) in PBS.

Free-floating sections were first preincubated (1 hour) in small Petri dishes containing 2% BSA in PBS, then incubated (2 hours) with the primary antibody diluted 1:100, and finally the sections were treated with the secondary antibody (e.g., antirabbit Ig coupled to FITC or HRP diluted 100-fold) for 2 hours. For controls we used nonimmune rabbit serum.

Peroxidase activity was revealed with diaminobenzidine (DAB) according to the method of Graham and Karnovsky (1966). Microscopic observations were carried out as previously described (Ghandour et al., 1980).

For electron microscopy, after the DAB reaction, the sections were washed in PBS and postfixed in 1% OsO_4 in 0.2 M cacodylate buffer, pH 7.2, for 30 minutes, briefly (3–5 minutes) washed in H_2O, dehydrated in ethanol, and finally embedded in Spurr resin. Uncounterstained ultrathin sections were observed with an EM 420 Philips.

RESULTS

Gallotia galloti, free in nature, mates at the end of April, lays eggs, and buries them underground in June;

depending on the temperature, the eggs hatch usually around the middle of August. Because of the weather the temperature vagary, the development of the embryo has variable duration and is thus defined in embryonic stages (from E1 to E40), not as time intervals. At E12 the neural fold begins to form, and at E24 the neural tube is completely closed. The telencephalon is formed between E24 and E30, when it separates from the diencephalon. At E32 cerebral hemispheres, septum and lateral ventricles are defined. A ventricular wall that is nine or ten cells thick is distinguishable at E30 and differentiates into the various ventricular zones and sulci starting from E32 (Yanes et al., 1988a,b).

Around E35-E36, a weak but clear GS immunoreactivity was detected in radial processes, in cell bodies in the ventricular walls, and in some scattered cell bodies (not shown) in mesencephalon. In telencephalon no GS immunoreactivity was detected until E36.

At E37 the staining intensity and number of the immunoreactive cells markedly increased in mesencephalic isthmic nuclei (Fig. 3A). In telencephalon, a weak staining appeared around the ventricles and in the ventricular walls, particularly in the sulci (not shown).

At E40 in mesencephalon the cell bodies in the ventricular wall (Figs. 1B, 3B), the radial fibers, and scattered cell bodies, particularly in the periventricular layer of the optic tectum and of the pretectal zone (Figs. 1A, 3C,D), were highly reactive. The presence of GS-positive cells that seemed to migrate out of the sulcus limitans was characteristic at this stage (Figs. 1B,D). These cells had round cell bodies and one major process aligned with radial fibers, which, at this stage were highly reactive (Fig. 2A, 3C). This major process often terminated on the wall of a blood vessel (Fig. 3E).

At the same age, the labelling greatly increased in telencephalon: positive "straight" radial fibers spread out of the ventralis, terminalis, and septomedialis sulci (Figs. 2A, 4C,E), whereas sinuous fibers radiated from the sulcus lateralis and crossed the ADVR (Figs. 2A, 4A,B) and the septal nuclei. Positive perivascular processes were detected in the ADVR (Fig. 4B). Another important feature at this embryonic stage are the star-shaped GS-positive cells, which now appeared in the striatum ventralis (Fig. 4F). Isolated, GS-positive, round or ovoid cell bodies located along the radial fibers, which spread from the sulcus septomedialis, were also abundant (Fig. 4C,D). These ovoid cells were close to the sulcus septomedialis.

At hatching, immunoreactive radial processes, cell bodies in the periventricular layer of the optic tectum, and dispersed cell bodies in midbrain central areas were observed (Figs. 1C,D, 5B). In the pretectum (Fig. 5A), immunoreactivity decreased in the radial fibers, but it increased in scattered cells in the tegmentum, particularly at the level of the oculomotor (Figs. 1C, 5C) and trochlear nuclei and in the optic tract (not shown). Numerous immunoreactive cells appeared to stream out of the sulcus limitans (Figs. 1D, 5D) (see Discussion). Dispersed immunoreactive cells were abundant in the nuclei profundus, ruber, oculomotor, and interpeduncularis in the rostral midbrain, and in the nuclei trochlearis, isthmi, and reticularis isthmi in the caudal midbrain.

In telencephalon, radial fibers were still intensely immunoreactive in all the areas in which they were observed at earlier ages (Fig. 6A,B,D), except in the sulcus septomedialis, where these fibers were less reactive (Fig. 6C). The number of isolated ovoid GS-positive cells in the sulcus septomedialis remained relatively low, whereas that of the star-shaped cells in the striatum ventralis (not shown) and, even more, in the commissura anterior (Fig. 6D) increased rapidly. Neurons appeared as unstained round spaces (Figs. 5C, 6C).

During development after hatching, the ependymal glial cells and radial fibers in the optic tectum and the wall of the 3rd ventricle remained immunoreactive, although intensity progressively decreased (Fig. 7A), whereas the scattered cells in every layer of the optic tectum (Figs. 1E,F, 7B) increased in intensity, particularly in the n. ruber (Figs. 1C,D, 7C), n. trochlearis, and n. oculomotorius (Figs. 1C, 7D), in the sulcus limitans (Fig. 7F), and in the torus semicircularis (Fig. 1E,F). The ependymal glial cells around the sulcus limitans and the cells that seemed to stream out of it were highly positive (Figs. 1D, 7F). In the optic tectum, the immunoreactive cells extended to the most superficial layers; at hatching they were limited to the central layers (Fig. 5B), and at E40 they were confined to the periventricular layer (Fig. 3C).

In telencephalon, immunoreactivity in the radial fibers and in the ependymal glial cells slightly decreased (Figs. 2B, 8A-C) and a clear-cut decreasing caudorostral gradient of the immunolabelling intensity was observed. This gradient was also present at earlier stages, but differences were not as striking as at this age. During this period, the migration of ovoid-shaped positive cells was also evident, as they progressively invaded the dorsal cortex from the sulcus septomedialis (Fig. 8B,C).

In adults, immunoreactivity in the ependymal glial cells decreased in the tectum and tegmentum, whereas it remained strong in dispersed cells in the n. oculomotorius (Figs. 1E, 9C), n. trochlearis and decussatio, n. interpeduncularis, n. profundus mesencephali (Figs. 1E, 9B), n. ruber, n. opticus tegmenti, torus semicircularis, n. isthmi, n. reticularis isthmi, and optic tract (Figs. 1E, 7E). These cells were thus present in all mesencephalic zones. The "migrating" cells were still detectable in the lateral zone of the Silvius aqueduct and above the oculomotor nucleus (Fig. 1E,F). Some immunoreactive cells appeared as satellite cells to blood vessels (Fig. 9D); also, ependymal glial cell processes appeared to contact capillary walls (Fig. 9A). Neurons in the different layers of the tectum were immunonegative (Fig. 9C).

In telencephalon, the immunoreactivity of ependymal glial cells and of radial fibers was weaker (Fig. 10A–D) than at earlier stages. Radial fibers, particularly those in the ADVR (Figs. 2C, 10A) and in the lateral cortex,

were weakly reactive and followed sinuous pathways. Scattered positive cells were abundant in defined zones. These were two types: star-shaped cells and ovoid cells. The former were abundant in the striatum ventralis (Fig. 10E), commissura anterior, and amygdaloid complex (Fig. 2C). The ovoid cells are more abundant near the sulcus septomedialis (Figs. 8B, 10D). Their ultrastructure corresponded to that of astrocytes (Figs. 8E, 10F). The cytoplasm of cell processes in the neuropil (Fig. 9F) and of pericapillary end-feet (Fig. 10F) were filled with peroxidase reaction product. In the cell bodies, immunoperoxidase precipitate was observed in the cytoplasm and ergastoplasmic cisternae (Figs. 8D,E, 10F) of cells, the nuclei of which had the features of astrocyte cell nuclei (Fig. 9E). Nuclei, nucleoli, mitochondria, and other organelles were free of immunopre-

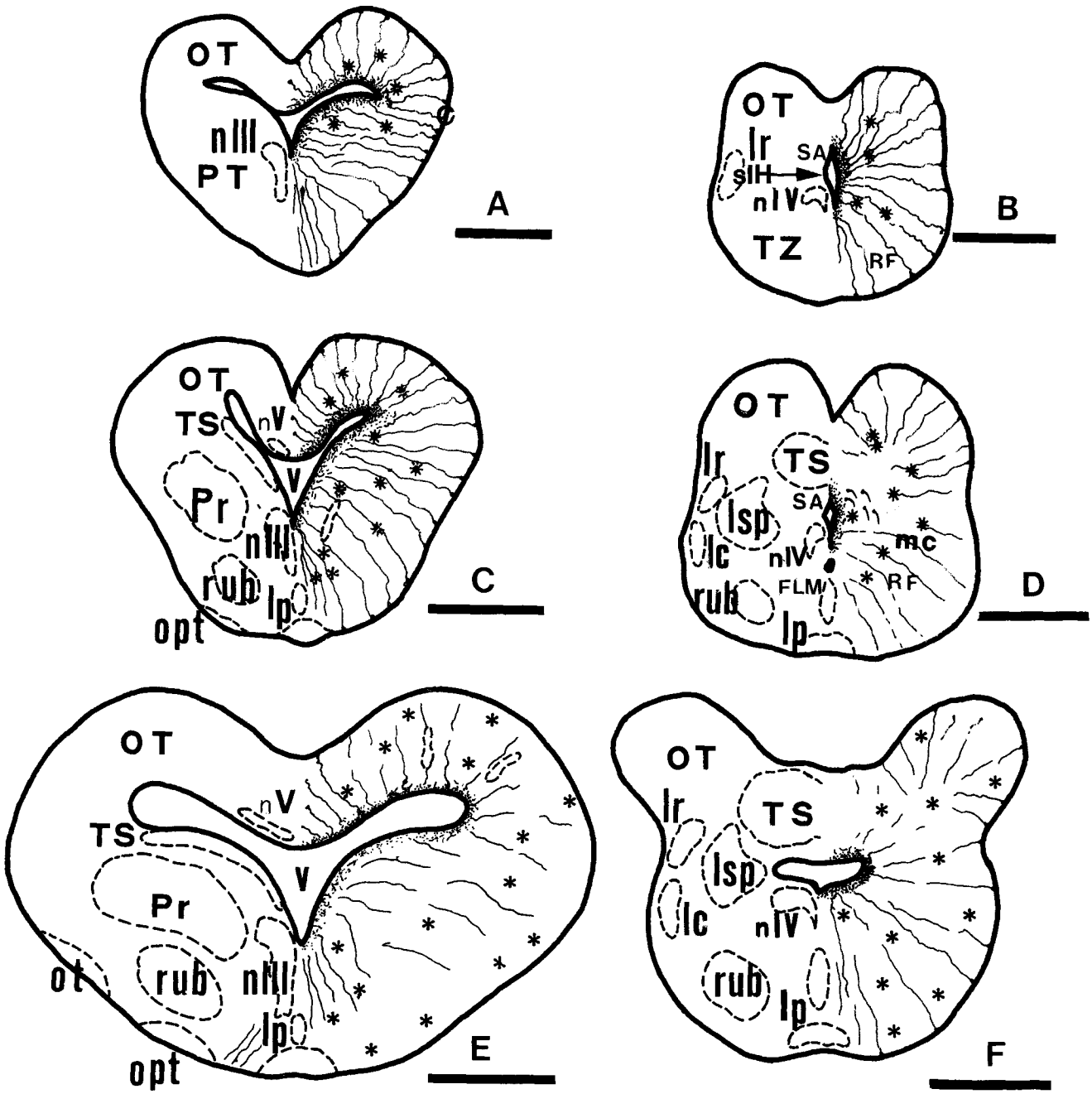

Fig. 1. Schematic drawing of *Gallotia galloti* mesencephalon sections at different developmental ages. In the left half of each section, the different areas, tracts, and nuclei are represented; in the right half, glutamine synthetase immunoreactive structures are drawn: scattered cells (*), radial fibers, and periventricular areas. A: Rostral levels, E40; B: caudal levels, E40; C: intermediate level at hatching; D: caudal level at hatching; E: intermediate level in adult; F: caudal level in adult. Scale bars = 1,000 μm.

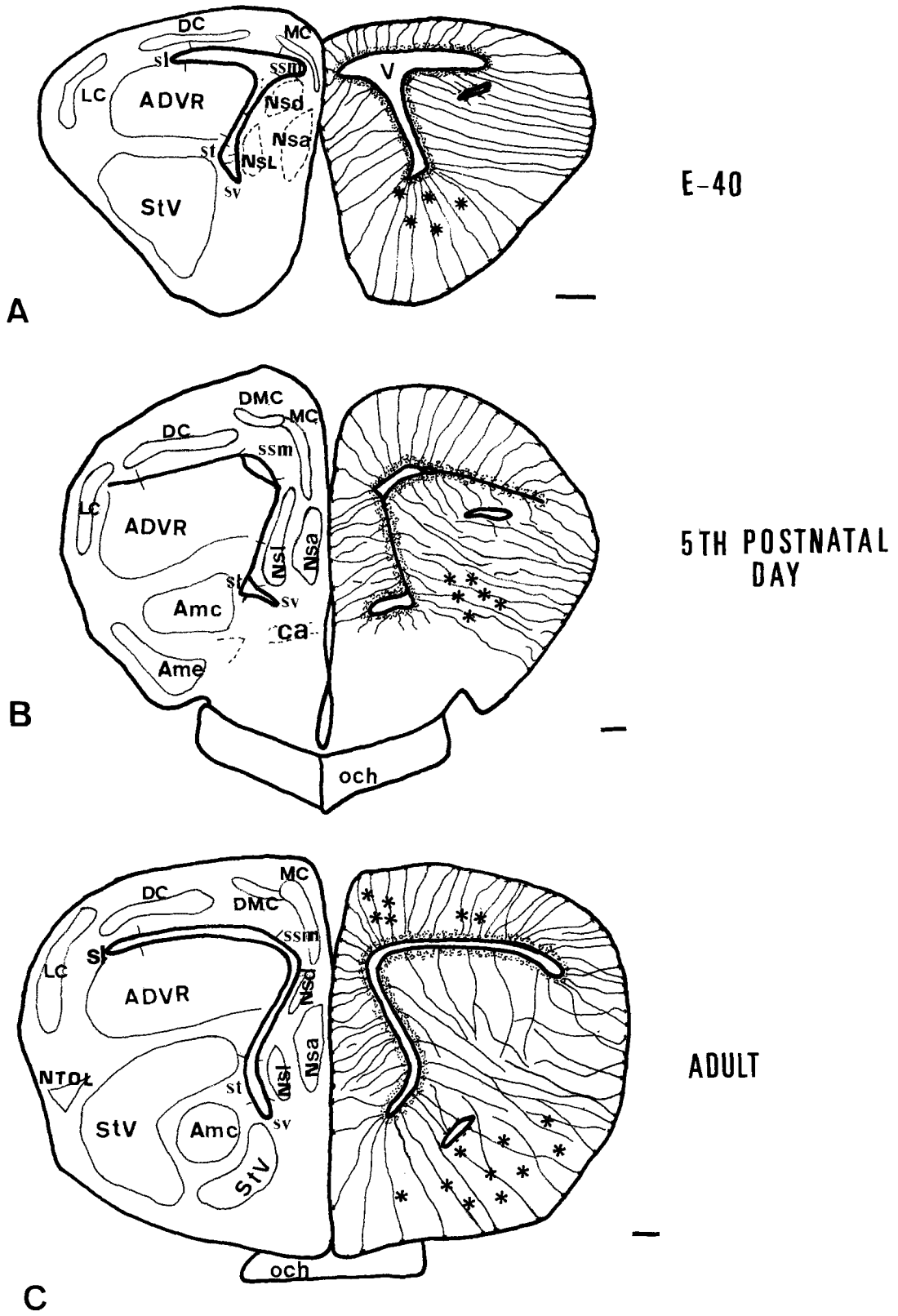

Fig. 2. Schematic drawing of *Gallotia galloti* telencephalon sections at different developmental ages. In the left half of each section, the different areas, tracts, and nuclei are represented; in the right half, glutamine synthetase immunoreactive structures are drawn: scattered cells (*), radial fibers, and periventricular areas. A: Rostral level at E40; B: mid-level on the 5th postnatal day; C: anterior level in adult. Scale bars = 200 μm.

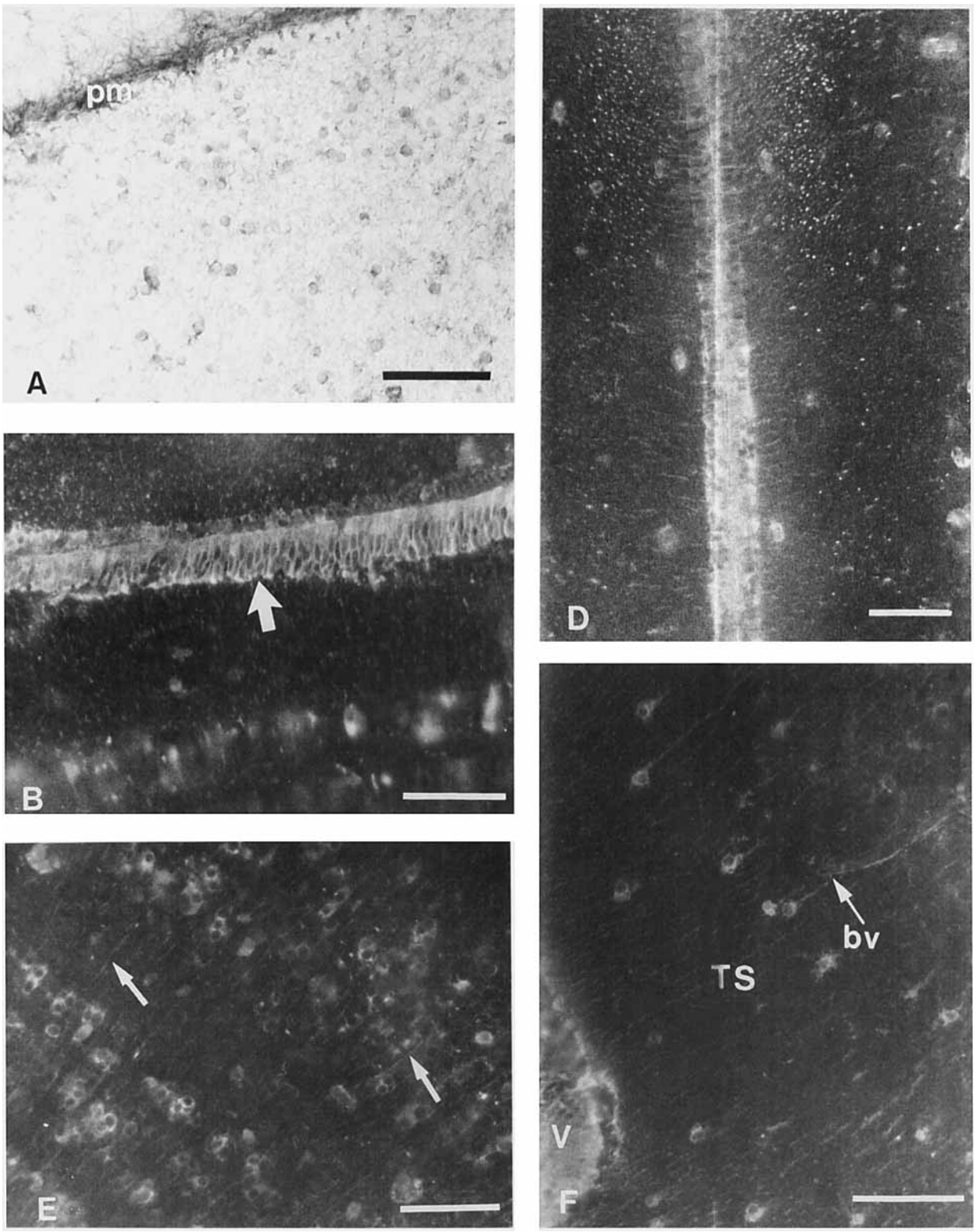

Fig. 3. Transverse sections of *Gallotia galloti* midbrain at embryonic stages 37 and 40 showing glutamine synthetase immunoreactivity as revealed by the immunoperoxidase method (A) and indirect immunofluorescence (B–E). **A:** Immunoreactive cell bodies in isthmic nuclei (pars rostralis) at E37; **B:** intense immunofluorescence in cell bodies of the ventricular wall (thick arrows) at E40; **C:** positive radial fibers (small arrows) and cell bodies in the periventricular layer on the optic tectum side at E40; **D:** the same as in C, but in the pretectum side. Notice the positive cells apparently "migrating" out of the ventricular zone at E40; **E:** cell bodies and perivascular glial processes (arrows) in the torus semicircularis at E40. Scale bars = 100 μm.

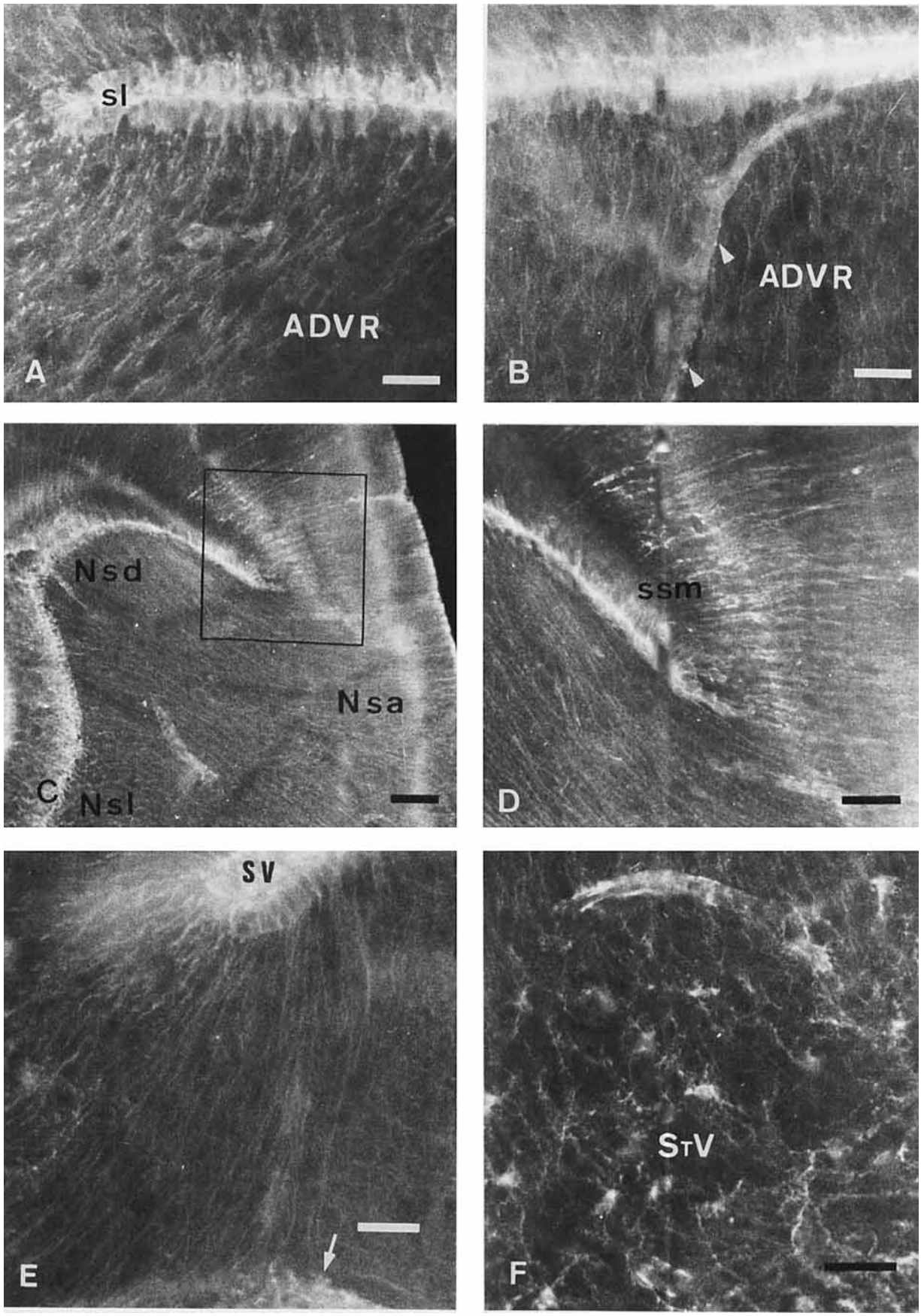

Fig. 4.

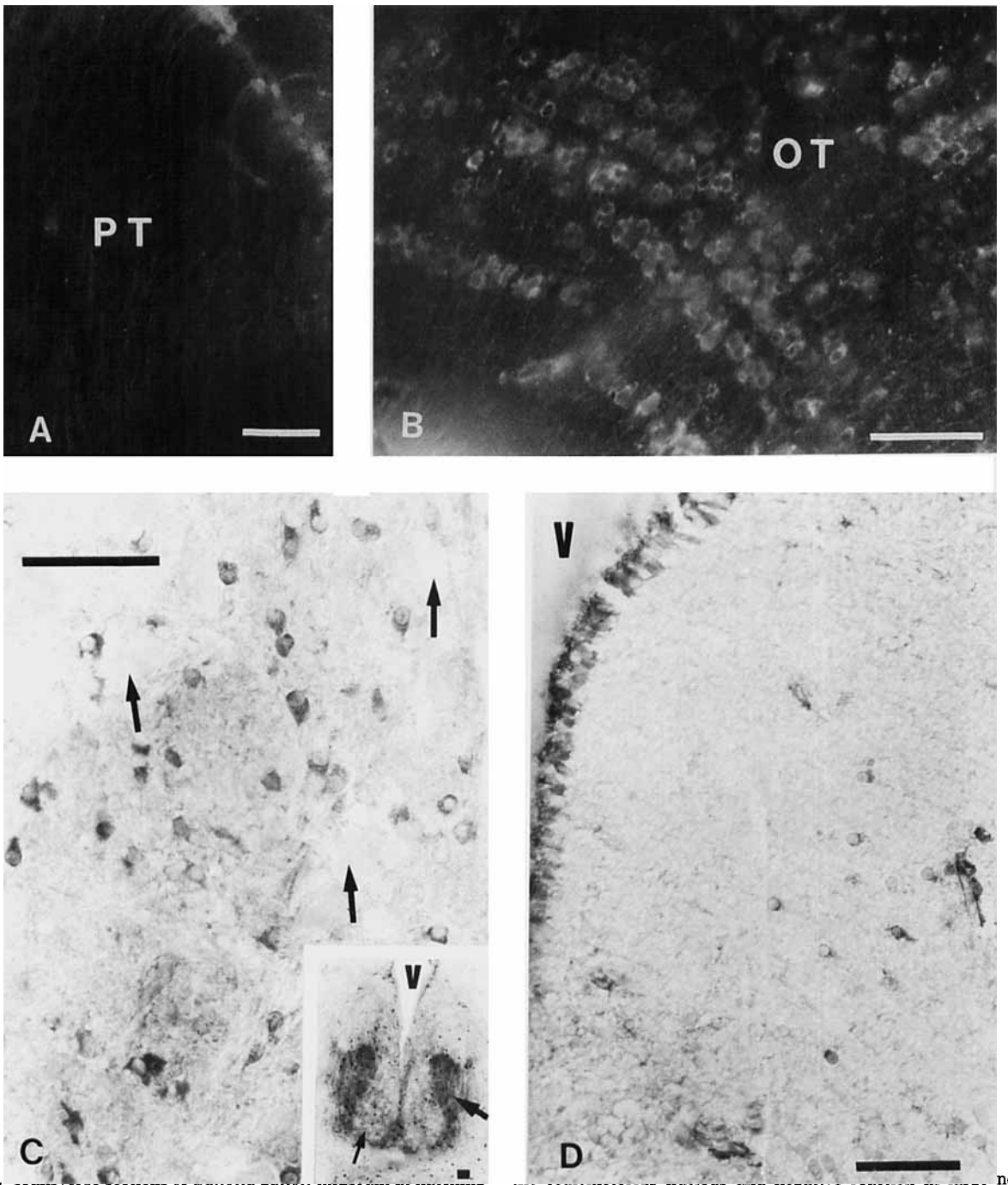

Fig. 5. ... neurons showing glutamine synthetase immunofluorescence (A,B) or immunoperoxidase (C,D). Weak immunoreactivity in cell bodies and radial fibers of the pretectum (A). In contrast, immunoreactivity is stronger than earlier in the periventricular and central layers and in dispersed cells in the optic tectum (B). C: Strong immunoreaction in round cells in (arrows). In the inset, oculomotorius nucleus (thin arrow) and fasciculus longitudinalis medialis (thick arrow) at low magnification. D: Strong immunoreaction in the ventricular wall near the sulcus limitans and scattered positive cells exhibiting one major process aligned with the radial fibers. Scale bars = 100 μm.

Fig. 4. Transverse sections of *Gallotia galloti* telencephalon at embryonic stage E40 (last embryonic stage before hatching) showing positive ependymal glial cells in the different sulci and positive radial fibers: s. lateralis (A), s. septomedialis at the rostral telencephalic level (C), corresponding to the insert but at a higher magnification (D), and s. ventralis (E). Note in A that the unstained neuronal cell bodies in the ADVR appear as dark spaces and in E the immunoreactive perivascular end-feet (arrow, E). B: Positive cell bodies in the periventricular layer near the ADVR. Note the sinuous paths of the immunofluorescent radial fibers and the apparent labelling of blood vessels due to the numerous glial end-feet on them (arrowheads). F: Striatum ventralis: Positive, star-shaped, dispersed cells, and their processes. Scale bars = A,B,D–F, 50 μm; C = 100 μm.

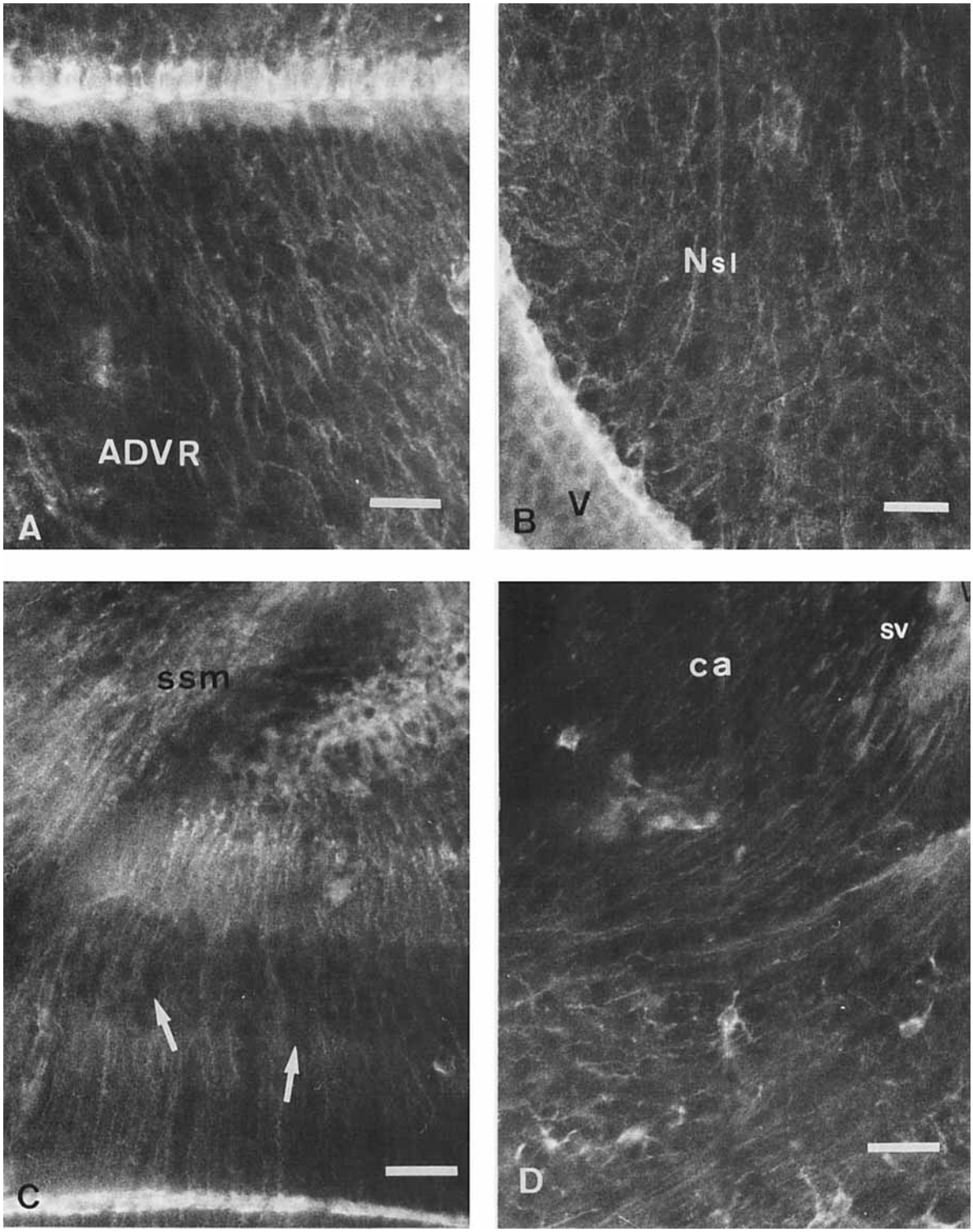

Fig. 6. Transverse sections of *Gallotia galloti* telencephalon at hatching showing glutamine synthetase immunofluorescence. Intense immunoreactivity in the ventricular wall on the side of the ADVR (A) and of the nucleus septalis lateralis at the telencephalon caudal level (B) and in the sulcus septomedialis (C); note the radial orientation of the fibers and their sinuous path in the ADVR (A) and the intensely positive fibers in (C). Note also the absence of scattered positive cells in (A), (B), and (C) and the presence of neurons, which appear as dark spaces (arrows) in (C). D: Dispersed, star-shaped, positive cell bodies and radial fibers in the commissura anterior and in the sulcus ventralis at the caudal level of telencephalon. Scale bars = 50 μm.

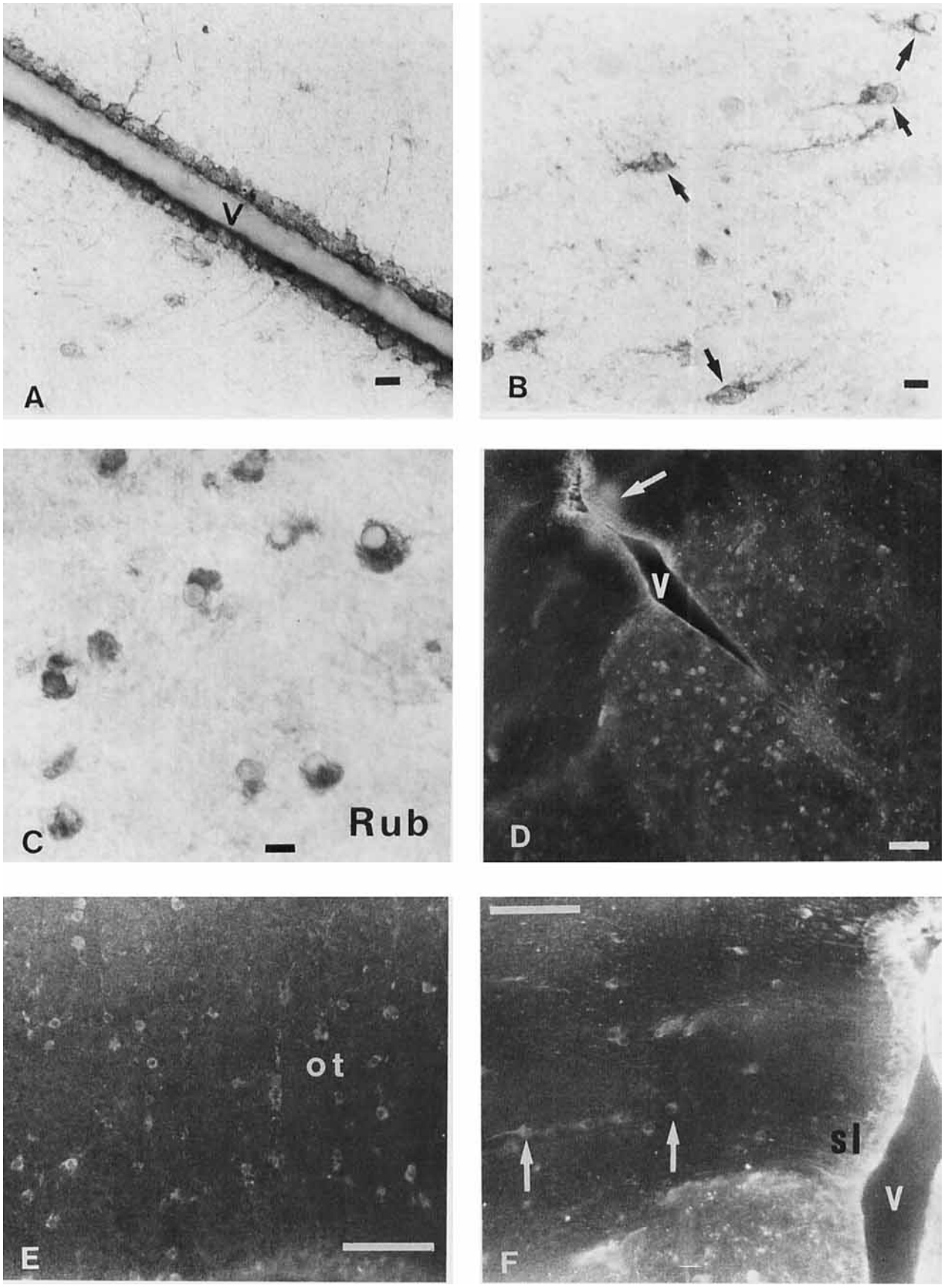

Fig. 7.

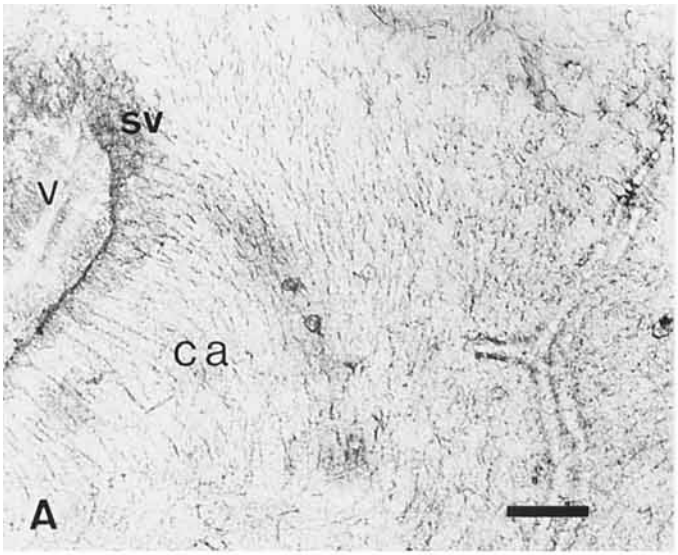

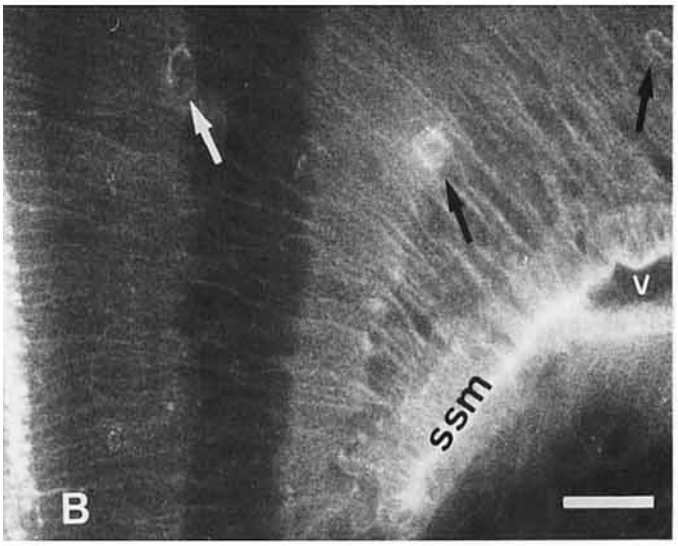

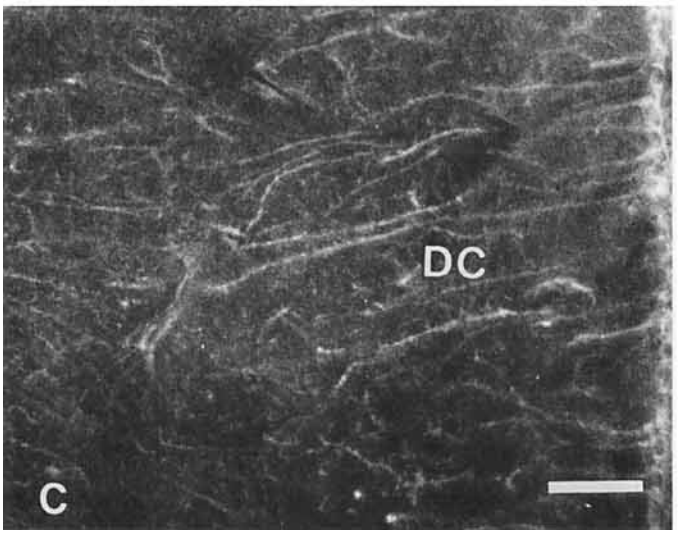

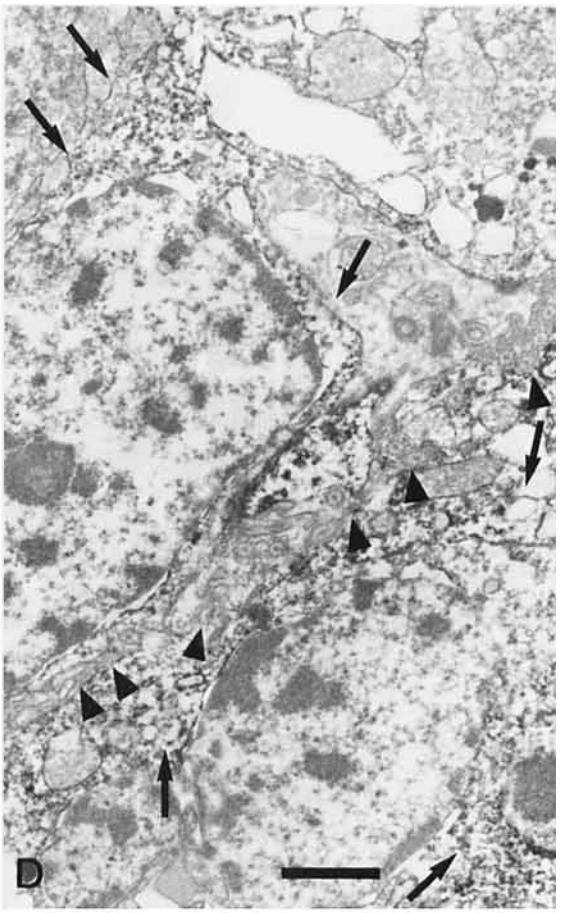

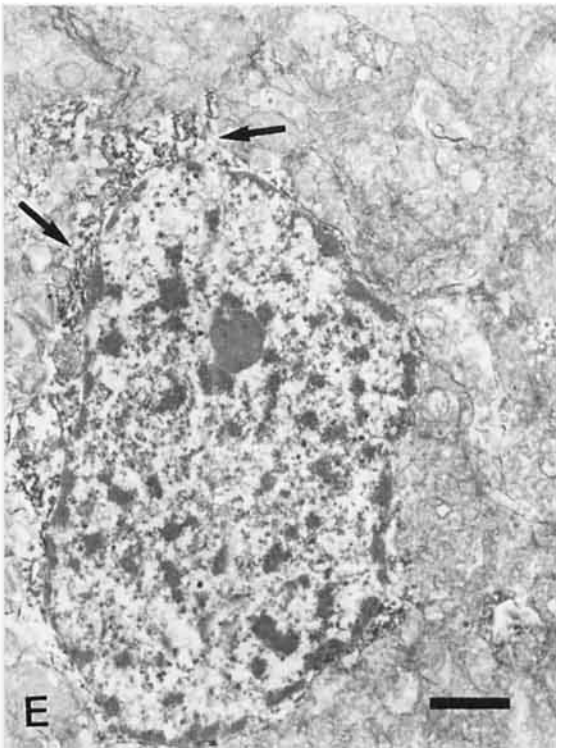

Fig. 8.

cipitate (Fig. 8D,E, 9E). Oligodendrocytes, pericytes, neurons (Fig. 9F), and endothelial cells (Fig. 10F) were not reactive. At all ages, no labelling could be detected in control sections.

DISCUSSION
Adults

Glutamine synthetase cell specificity

In the adult *Gallotia galloti* telencephalon and mesencephalon, GS is present in radial glial processes and in ependymal glial cell bodies. This cellular distribution is the same as that of GFAP (Monzon et al., 1989; Yanes et al., 1989) although in subpial end-feet GS immunoreactivity is less intense than that of GFAP.

GS-positive star-shaped cells with the morphology of typical astrocytes are abundant in the striatum ventralis, amygdaloid complex, and commissura anterior, but they are absent in the whole mesencephalon.

Additional GS-positive ovoid or pear shaped cells (as indicated by immunofluorescence or HRP stain) are scattered throughout mesencephalon and telencephalon. The ultrastructural features of the cell nucleus of these "ovoid" cells (Fig. 9E) and the presence of processes originating from their cell bodies and terminating as end-feet on blood vessels (Fig. 10F) suggest that they are astrocytes. Doubts on their astrocytic nature could be raised on account of the shape of their soma; however, the absence of a star-like shape alone is not a sufficient criterion for doubting the astrocytic nature of these cells, since their shape is the same as that of some GFAP-positive cells in *Gallotia galloti* (Monzon et al., 1989; Yanes et al., 1989) and the GS-positive astrocytes in chick cerebellum (Tholey et al., 1987a). All of this concurs to indicate that the ovoidal cells are astrocytes.

Simultaneous presence of GS and GFAP

In telencephalon, the cellular specificity of GS immunoreactivity was similar but not identical to that of GFAP (Yanes et al., 1989). In general, ependymal glial cell bodies and radial processes are GFAP- and GS-positive, but in the medial cortex we did not detect GS-positive fiber bundles with the same orientation (e.g., parallel to the ventricular wall) as GFAP-positive fiber bundles (Yanes et al., 1989); thus, some fibers are GS-negative/GFAP-positive. Conversely, numerous GS-positive cells were observed in areas where GFAP-positive cells were practically absent such as the dorsomedial cortex, amygdaloid complex, and striatum ventralis. In the striatum ventralis, however, GFAP-positive processes were detected (Yanes et al., 1989), which probably originate from the GFAP-positive/GS-positive ependymal glial cell bodies.

Also, in all midbrain areas, GS-positive ovoid cells are much more abundant than the GFAP-positive cells in the same area (Monzon et al., 1989; Yanes et al., 1989); thus, most midbrain astrocytes must be GS-positive and GFAP-negative.

It appears thus that not all astrocytes in the adult *Gallotia galloti* are GFAP-positive. In addition, the distribution of cell bodies and fibers suggests that the astrocytes in this lizard express different combinations of GS and GFAP. Previous observations on vimentin in some astrocytic processes in adult mesencephalon (Monzon et al., 1989) may further complicate the picture, since vimentin occurs in areas where no GFAP-positive cells bodies were detected and where GS-positive cells appear to be abundant. These processes probably belong to radial glia, but they indicate the possibility of the presence of either vimentin-positive/GS-positive/GFAP-positive cell processes or of vimentin-positive/GS-positive/GFAP-negative cell processes. Evidently, double-labelling experiments with two antibodies at the time are necessary to confirm these points. The absence of GFAP, and possibly vimentin, raises the question of the type of intermediate filaments, if any, present in the GS-positive cells.

Astrocytes preferentially or exclusively expressing either GS or GFAP have already been described. Hallermayer and Hamprecht (1984) described GS-negative rat astrocytes in primary cultures, whereas Patel et al. (1985) reported that the ratio between GFAP and GS varied in the different regions of the adult rat CNS.

Fig. 7. Transverse sections of *Gallotia galloti* midbrain after hatching (5th postnatal day) showing glutamine synthetase immunoreactivity as revealed by the immunoperoxidase method (A,B,C) or indirect immunofluorescence (D,E,F). **A:** Strongly labelled cell bodies in the 3rd ventricle wall and weakly immunoreactive radial fibers. Strongly stained scattered cells in optic tectum (B), red nucleus (C), oculomotorius nucleus (D), optic tract (E), and apparently migrating out of the sulcus limitans (arrows, F). In D the arrow points to the sulcus limitans. Scale bars = A–C, 10 μm; D–F, 100 μm.

Fig. 8. Transverse sections of *Gallotia galloti* telencephalon at the 5th postnatal day showing glutamine synthetase immunoreactivity as revealed by indirect immunofluorescence in optical microscopy (B,C) and by the immunoperoxidase reaction in optical (A) and electron (D,E) microscopy. **A:** Positive ependymal glial cells in the sulcus ventralis; **B:** in the sulcus septomedialis; **C:** in the ventricular wall facing the dorsal cortex and their straight or sinuous radial processes. Note the isolated positive cells at the level of the commissura anterior in (A) and in (B) (arrows) and the absence of these cells in (C). **D:** Electronmicrograph of positive ependymal glial cells (arrows) along the virtual cavity of the ventricle (ventricular coarctation indicated by arrows heads) at the level of the sulcus ventralis. The immunolabel is restricted to the cytoplasm. The nucleus appears clear with dispersed peripheral chromatin, typical of astrocytes. **E:** Electronmicrograph of an isolated positive cell in the nucleus centralis amygdalae. Note the immunolabel in the cytoplasm of the cell (arrows). The nucleus appear to be that of an astrocyte. Scale bars: A–C, 50 μm; D,E, 1 μm.

Fig. 9. Transverse sections of adult *Gallotia galloti* midbrain showing glutamine synthetase immunoreactivity as revealed by indirect immunofluorescence by optical microscopy (A–D) and immunoperoxidase reaction by electron microscopy (E,F). **A:** Immunoreactive radial cell in the ventricular wall and fibers in the optic tectum. Note the end-feet on a blood vessel. Bar = 100 μm. Positive cell bodies scattered through the nucleus profundus mesencephali (**B**) and the nucleus oculomotorius (C) and satellite to blood vessels (**D**). Note the radial fibers in the tegmentum (C). Bar = 100 μm. **E:** Peroxidase immunoprecipitate in an astrocyte cytoplasm and ergastoplasmic cisternae (arrows). The nucleus and other organelles are negative. Bar = 1 μm. **F:** Immunopositive astroglial processes (arrows) in the neuropil and immunonegative neurons. Bar = 1 μm.

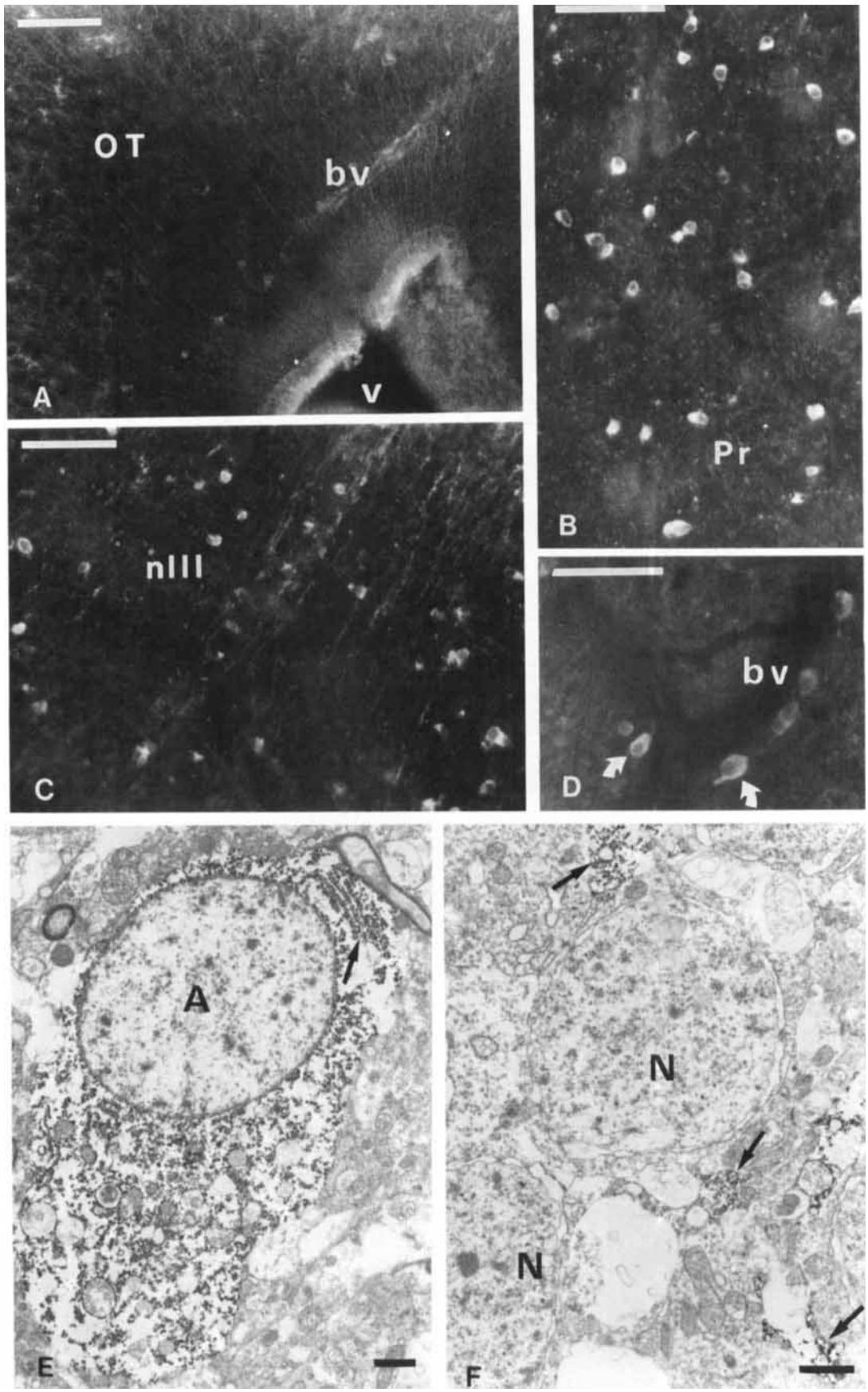

Fig. 9.

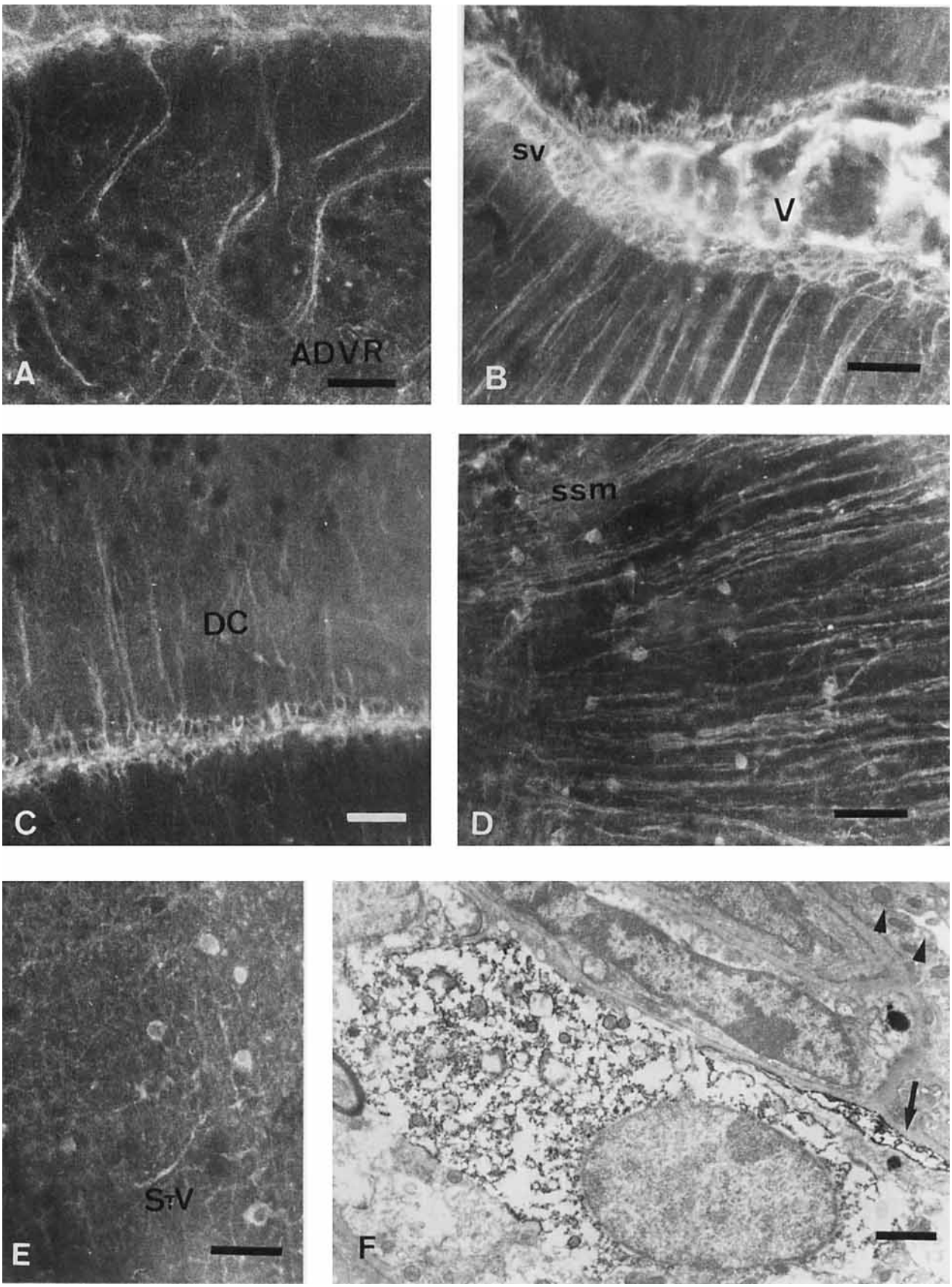

Fig. 10.

GFAP-negative/GS-positive astrocytes have been observed in rat brain (Didier et al., 1986). Linser (1985) has shown that the distribution of GFAP- and GS-positive cells in the different layers of avian optic tectum is different from that of GFAP-negative/GS-positive cells. The GFAP-negative/GS-positive cells are protoplasmic astrocytes, although they apparently contain also carbonic anhydrase II, which in mammals is an oligodendrocyte marker. Norenberg (1983), using an antisheep GS antiserum, has shown the presence of GFAP-negative/GS-positive ependymoglial cells in toad and goldfish. Kriegstein et al. (1986), using a monoclonal antibody raised against turtle glial cells and an anti-GFAP immunoserum, described the presence of GFAP-negative astrocyte cell bodies in turtle striatum. This indicates that the diversity of astrocyte marker expression is much more evident in birds and reptiles than in mammals.

Another species-specific difference in astrocyte distribution in reptiles is that star-shaped GFAP-positive cell bodies are absent in turtle but present in snake telencephalon (Onteniente et al., 1983); in this lizard, they are absent in telencephalon but present in mesencephalon. Our present results not only agree with our previous suggestion that, as far as glial evolution is concerned, Lacertidae occupy a position in phylogeny between Ofidiae and Testudo (Yanes et al., 1989) but, in addition, suggest that Lacertidae are closer to Testudo than to Ofidia.

Functional implications

The different expression of astrocytic markers in astrocytes in different anatomical sites or in different subcellular compartments may have functional implications; for example, in view of the fact that the enzymatic activity of astrocytic GS is essential for the glutamatergic neurotransmission in mammals (Hamberger et al., 1979), astrocytes near glutamatergic circuits might be the richest in GS. There is one example of such a functional specialization of astrocytes in rodent cerebellum: Bergman glia, present in the cerebellar molecular layer where the glutamatergic neurotransmission network is dense, takes up glutamate by a very high-affinity system; this is not the case for astrocytes located in the cerebellar granular layer (de Barry et al., 1983). In the case of *Gallotia galloti,* there is no information on glutamatergic neurotransmission in lizard CNS, and a mapping of glutamatergic neurons would be necessary.

Miller and Liuzzi (1986) observed that the processes of glial cells located near myelinated fibers were particularly rich in GFAP-positive intermediate filaments. Even though the reason and the meaning of this abundance of gliofibrills are not known, this appears to be a general property of the astrocytes localized in myelinated axonal bundles.

Ontogeny

During embryonic development, GS immunoreactivity appears in ependymal glial cell bodies and in radial glial processes at about the same time as, or slightly after, that of GFAP (thus later than that of vimentin), and it increases in parallel with the formation and maturation of ependymal and radial glia. This is a general feature of glial maturation, since it was also observed in mammalian astrocytes in vivo and in cultures in vitro (Patel, 1986). Topographically, GS, like GFAP, appears in a caudorostral progression of astrocyte maturation during development (Table 1).

After hatching, GS immunoreactivity clearly decreased, particularly in radial fibers, but it is unclear if the regression of GS immunoreactivity is due to a reduction of the cellular GS concentration or to a decrease of the number of GS-positive ependymal glial cell bodies or both. We can suppose that during cell multiplication, when the need for amino groups for the synthesis of nucleic acid bases is high, the need for glutamine is also high; thus, sustained GS activity is necessary. In this case radial glial fibers, besides having

TABLE 1. Schematic representation of the average immunoreactivity in ependymal glia, radial fibers, and glia limitans when antibodies directed against vimentin and glial fibrillary acidic protein and glutamine synthetase were used (A) and of the presence during development of scattered astrocytes exhibiting immunolabelling with the different antibodies (B)[a]

	Mesencephalon			Telencephalon		
	VIM	GFAP	GS	VIM	GFAP	GS
A						
E 32	+			+		
E 34	+++	±		+++		
E 35	+++	+	±	+++		
E 36	++	++	±	++	±	±
E 40	+	++	++	+	++	+
Hatching	#	+++	+++		++	++
PND 5	#	+++	++		++	+++
Adult	#	+++	+		++	+
B						
E 32						
E 34						
E 35	*		*			
E 36	*		*			
E 40	*		*			*
Hatching			*			*
PND 5		*	*			*
Adult		*	*			*

[a]GFAP = glial fibrillary acidic protein; GS = glutamine synthetase; VIM = vimentin. The arbitrary scale is from very weak (±) to very strong (+++). # = persistence of vimentin reactivity in some perivascular and subpial end-feet. * = immunolabelling by different antibodies. Note the constant absence of VIM- and GFAP-positive scattered astrocytes in telencephalon. (*Adapted from Monzon-Mayor et al., 1989; Yanes et al., 1989c.*)

Fig. 10. Transverse sections of adult *Gallotia galloti* telencephalon showing glutamine synthetase immunoreactivity as revealed by indirect immunofluorescence in optic microscopy (A–E) and immunoperoxidase reaction in electron microscopy (F). **A:** Positive ependymal cells in the ventricular walls near the ADVR, in the sulcus ventralis (**B**), and near the dorsal cortex (C). Positive radial fibers are sinuous in (A) and straight in (B) and (C). No dispersed positive cells are detected in any of these areas. In contrast, numerous immunoreactive cell bodies and their processes are dispersed between radial fibers originating from the sulcus septomedialis (D) and in the striatum ventralis (E). The cell processes of the dispersed cells appear to be aligned along the radial fibers (D). F: Electronmicrograph of an isolated positive dispersed cell in the striatum ventralis. The immunoprecipitate is localized in the cytoplasm. The cell nucleus is typical of an astrocyte. Note also the positive perivascular end-foot (arrow) and the negative vascular endothelial cells (arrowheads). Scale bars = A–E, 50 μm; F : 1 μm.

a role in cell migration, may also contribute to cell formation by supplying the needed glutamine to mitotic cells. When cell multiplication is finished, the need for glutamine decreases; hence high GS activity is no longer required, and GS concentration decreases in radial glia. Alternatively or concurrently, a decrease in the number of GS-positive ependymal glial cell bodies can occur because they migrate out of the periventricular zone. This migration is suggested by the fact that ovoid GS-positive cells appear at E40 along the path of radial fibers, at first around the sulci in the Silvius aqueduct (Fig. 1B); at hatching these cells have spread, always along radial fibers, in the optic tectum and pretectum to more than halfway toward the pial surface (Figs. 1C,D). At later ages, these cells are present in the whole depth of the midbrain. In telencephalon, ovoid GS-positive cells appear to migrate out of the sulcus septomedialis. Ramón y Cajal (1911) hypothesized that both astrocytes and ependymocytes derive from radial glia, and more recently Choi et al. (1983) and Levitt and Rakic (1980) have shown that during mammalian development radial glial cells are transformed into astrocytes through a "transitional cell type" stage until at birth, when radial glia has disappeared. In mammals both astrocytes and radial glia are GFAP-positive; ependymocytes are GFAP-negative, although they do express other astrocyte markers such as S-100 protein (De Vitry et al., 1980; Didier et al., 1986). Ependymal glial cells and radial processes in *Gallotia galloti* are GFAP- (and GS-) positive; thus, the scattered GS-positive/GFAP-negative cells in *Gallotia galloti* midbrain apparently are not equivalent to the "transitional" cells in mammalian brain, since they do not further differentiate. They may represent another choice during phylogeny of the evolution of radial glia into a particular type of astrocyte.

In contrast to the ovoid cells, the earliest star-shaped GS-positive cells in telencephalon appeared in situ in the striatum or in the amygdaloid complex with no indication of migration nor of precursors (i.e., vimentin-positive and/or GFAP-positive cell bodies) in the same areas (Yanes et al., 1989). Possibly these cells migrated out of the ependymal zone and reached their adult position before expressing GS. Because the ultrastructure of these star-shaped cells is that of astrocytes, we think that, in spite of the absence of GFAP immunoreactivity, they represent a specialized type of astrocytes.

ACKNOWLEDGMENTS

Drs. M. Monzon-Mayor and C. Yanes Mendez were recipients of travel and research fellowships granted by the Convenio de Colaboracion Gobierno de Canarias-Caja General de Ahorros de Canarias (Canary Islands) and Ministerio de Educacion y Ciencia de Madrid (Spain). This work was partially supported by the research grant 909 (2) and PB87-0688-CO2-O2 from CAICYT. GG is DR II in CNRS and J. de B. is CR I in INSERM. The authors are grateful to Mrs. Yolande Schladenhaufen for her technical assistance and thank Dr. Francesco Vitiello for helpful discussion.

REFERENCES

Bignami, A. and Dahl, D. (1974) Astrocyte-specific protein and neuroglial differentiation. An immunofluorescence study with antibodies to the glial fibrillary acidic protein. *J. Comp. Neurol.*, 153:27–38.

Bischoff, W. (1982) Die innerntriche gliederung von *Gallotia galloti* (Dumeril Bibron, 1839) (Reptilia, Sauria: Lacertidae) Auf Tennriffa, Kanarische Inseln. Bonn. *Zool. Beitr.* 33:363–381.

Bloch, S., Ledig, M., Mandel, P., and Tholey, G. (1984) Purification et caractérisation de la glutamine synthetase de cerveau de Poulet. *Comptes Rendus. Acad. Sci. Paris (Serie III)*, 298:127–130.

Caldani, M., Rolland, B., Fages, C., and Tardy, M. (1982) Glutamine synthetase activity during mouse brain development. *Experientia*, 38:1199–1202.

Choi, B.H., Kim, R.C., and Lapham, L.W. (1983) Do radial glia give rise to both astroglial and oligodendroglial cells? *Dev. Brain. Res.*, 8:119–130.

Dahl, D. and Bignami, A. (1973) Immunochemical and immunofluorescence studies of the glial fibrillary acidic protein in vertebrates. *Brain Res.*, 61:279–293.

Dahl, D., Crosby, C.J., Sethi, J.S., and Bignami, A. (1985) Glial fibrillary acidic (GFA) protein in vertebrate: Immunofluorescence and immunoblotting study with monoclonal and polyclonal antibodies. *J. Comp. Neurol.*, 239:75–88.

De Barry, J., Ghandour, M.S., and Gombos, G. (1983) Developing rat cerebellum: Glutamine and glutamate influx correlated with the cellular distribution of glutamine synthetase. *Int. J. Dev. Neurosci.*, 8:351–360.

De Vitry, F., Picart, R., Jacquet, C., Legault, L., Dupouey, P., Tixier-Vidal, A. (1980) Presumptive common precursor for neuronal and glial cell lineages in mouse hypothalamus. *Proc. Natl. Acad. Sci. U.S.A.*, 77:4165–4169.

Didier, M., Harandi, M., Aguera, M., Bancel, B., Tardy, M., Fages, C., Calas, A., Stagaard, M., Mollgard, K., and Belin, M.F. (1986) Differential immunocytochemical staining for glial fibrillary acidic (GFA) protein, S-100 protein and glutamine synthetase in the rat subcommissural organ, nonspecialized ventricular ependyma and adjacent neuropil. *Cell Tissue Res.*, 245:343–351.

Dufaure, J.P. and Hubert, J. (1961) Table de developpement du lézard vivipare *(Lacerta vivipara jacquin). Arch. Anat. Microsc. Morphol. Exp.*, 50:309–327.

Ghandour, M.S., Vincendon, G., and Gombos, G. (1980) Astrocyte and oligodendrocyte distribution in adult rat cerebellum: An immunohistological study. *J. Neurocytol.*, 9:637–646.

Graham, R.C. and Karnovsky, M.J. (1966) The early stages of absorption of injected horseradish peroxidase in the proximal tubules of mouse kidney. Ultrastructural cytochemistry by a new technique. *J. Histochem. Cytochem.*, 14:291–302.

Hallermayer, K., Harmening, G., and Hamprecht, B. (1981) Cellular localization and regulation of glutamine synthetase in primary cultures of brain cells from newborn mice. *J. Neurochem.*, 37:43–52.

Hallermayer, K. and Hamprecht, B. (1984) Cellular heterogeneity in primary cultures of brain cells revealed by immunocytochemical localization of glutamine synthetase. *Brain Res.*, 295:1–11.

Hamberger, A., Han Chiang, G., Nylen, E.S., Scheff, S.W., and Cotman, C.W. (1979) Evaluation of glucose and glutamine as precursors for the synthesis of preferentially released glutamate. *Brain Res.*, 168:513–530.

Juurlink, B., Schousboe, A., Jorgensen, O.S., and Hertz, L. (1981) Induction by hydrocortisone of glutamine synthetase in mouse primary astrocyte cultures. *J. Neurochem.*, 36:136–142.

Kriegstein, A.R., Shen, M., and Eshar, N. (1986) Monoclonal antibodies to the turtle cortex reveal neuronal subsets, antigenic cross-reactivity with the mammalian neocortex and forebrain structures sharing a pallial derivation. *J. Comp. Neurol.*, 254:330–340.

Levitt, P. and Rakic, P. (1980) Immunoperoxidase localization of glial fibrillary acidic protein in radial glial cells and astrocytes of the developing rhesus monkey brain. *J. Comp. Neurol.*, 193:815–840.

Linser, P.J. (1985) Multiple marker analysis in the avian optic tectum reveals three classes of neuroglia and carbonic anhydrase-containing neurons. *J. Neurosci.*, 5:2388–2396.

Ludwin, S.K., Kosek, J.C., and Eng, L.F. (1976) The topographical distribution of S-100 and GFA proteins in the adult rat brain: An immunohistochemical study using horseradish peroxidase labeled antibodies. *J. Comp. Neurol.*, 165:197–208.

Martinez-Hernandez, A., Bell, K.P., and Norenberg, M.D. (1977) Glu-

tamine synthetase: Glial localization in brain. *Science,* 195: 1356–1358.

Miller, R.H. and Liuzzi, F.J. (1986) Regional specialization of the radial glial cells of the adult frog spinal cord. *J. Neurocytol.,* 15:187–196.

Monzon-Mayor, M., Yanes, C., Ghandour, M.S., de Barry, J., and Gombos, G. (1989) GFAP and vimentin immunohistochemistry in the adult and developing midbrain of the lizard *Gallotia galloti. J. Comp. Neurol.* (in press).

Moscona, A.A. and Piddington, R. (1966) Stimulation by hydrocortisone of premature changes in the development pattern of glutamine synthetase in embryonic retina. *Biochem. Biophys. Acta,* 121: 409–411.

Norenberg, M.D. (1979) The distribution of glutamine synthetase in the rat central nervous system. *J. Histochem. Cytochem.,* 27:756–762.

Norenberg, M.D. (1983) Immunohistochemistry of glutamine synthetase. In: *Glutamine, Glutamate, and GABA.* L. Hertz, E. Kvamme, E.G. McGeer, and A. Schousboe, eds. Alan R. Liss, New York, pp. 95–111.

Norenberg, M.D. and Martinez-Hernandez, A. (1979) Fine structural localization of glutamine synthetase in astrocytes of rat brain. *Brain Res.,* 161:303–310.

Onteniente, B., Kimura, H., and Maeda, T. (1983) Comparative study of the glial fibrillary acidic protein in vertebrates by PAP immunohistochemistry. *J. Comp. Neurol.,* 215:427–436.

Patel, A.J., Hunt, A., and Tahourdin, C.S.M. (1983a) Regional development of glutamine synthetase activity in the rat brain and its association with the differentiation of astrocytes. *Dev. Brain Res.,* 8:31–37.

Patel, A.J., Hunt, A., and Tahourdin, C.S.M. (1983b) Regulation of in vivo glutamine synthetase activity by glucocorticoids in the developing rat brain. *Dev. Brain Res.,* 10:83–91.

Patel, A.J. and Hunt, A. (1985) Observations on cell growth and regulation of glutamine synthetase by dexamethasone in primary cultures of forebrain and cerebellar astrocytes. *Dev. Brain Res.,* 18:175–184.

Patel, A.J., Weir, M.D., Hunt, A., Tahourdin, C.S.M., and Thomas, D.G.T. (1985) Distribution of glutamine synthetase and glial fibrillary acidic protein and correlation of glutamine synthetase with glutamate decarboxylase in different regions of the rat central nervous system. *Brain Res.,* 331:1–9.

Patel, A.J. (1986) Development of astrocytes: In vivo studies. In: *Advances in the Biosciences, Vol. 61, Dynamic Properties of Glial Cells: Cellular and Molecular Aspects.* T. Grisar, G. Frank, L. Hertz, M. Sensenbrenner, and D.M. Woodbury, eds. Pergamon Press, Oxford, pp. 87–96.

Ramos, A. (1980) Tabla de desarrollo embrionario de Lacerta *Gallotia galloti* (periodo de embiogenesis) y aspectos de su reproduccion. Memoria de Licenciatura. Univ. La Laguna. Tenerife. Canary Islands, Spain.

Ramon y Cajal, S. (1911) *Histologie du Systeme Nerveux de l'Homme et des Vertebres.* Maloine, Paris.

Riepe, R.E. and Norenberg, M.D. (1977) Müller cell localization of glutamine synthetase in rat retina. *Nature,* 268:654–655.

Sena, A., Ferret-Sena, V., Sarlieve, L.L., and Tholey, G. (1988) Differential modulation of glutamate metabolizing enzymes in mouse and chick cultured glial cells by insulin. *J. Neurosci. Res.,* 20:189–194.

Schousboe, A., Svenneby, G., and Hertz, L. (1977) Uptake and metabolism of glutamate in astrocytes cultured from dissociated mouse brain hemispheres. *J. Neurochem.,* 29:999–1005.

Tardy, M., Rolland, B., Fages, C., and Caldani, M. (1984) Astroglial cells: Glucocorticoid target cells in the brain. *Clin. Neuropharmacol.,* 7:296–302.

Tholey, G., Ledig, M., Bloch, S., and Mandel, P. (1985) Glutamine synthetase and energy metabolism enzymes in cultured chick glial cells: Modulation by dibutyryl cyclic AMP, hydrocortisone, and trypsinization. *Neurochem. Res.,* 10:191–200.

Tholey, G., Bloch, M., Ledig, M., Mandel, P., and Wedler, F. (1987a) Chick brain glutamine synthetase and Mn^{2+}-Mg^{2+} interactions. *Neurochem. Res.,* 12:1041–1047.

Tholey, G., Ghandour, M.S., Bloch, S., Ledig, M., and Mandel, P. (1987b) Glutamine synthetase and energy metabolism enzymes in cultivated chick neurons and astrocytes: Modulation by serum and hydrocortisone. *Dev. Brain Res.,* 31:73–81.

Weil-Malherbe, H. (1962) Ammonia metabolism in the brain. In: *Neurochemistry,* 2nd ed. K.A.C. Elliot, I.H. Page, and J.H. Quastel, eds. Charles C. Thomas, Springfield, IL, pp. 321–330.

Yanes Mendes, C., Martin Trujillo, J.M., Perez Batista, M.A., Monzon-Mayor, M., and Marrero, A. (1988a) Ependymogenesis of the lizard basal areas. I. Ependymal zones. *Z. mikrosk.-anat. Forsch. Leipzig,* 102:555–572.

Yanes Mendes, C., Martin Trujillo, J.M., Perez Batista, M.A., Monzon-Mayor, M., and Marrero, A. (1988b) Ependymogenesis of the lizard basal areas. II. Sulcus. *Z. mikrosk.-anat. Forsch. Leipzig,* 102: 573–589.

Yanes, C., Monzon-Mayor, M., Ghandour, M.S., de Barry, J., and Gombos, G. (1989) Radial glia and astrocytes in the adult and developing telencephalon of the lizard *Gallotia galloti* as revealed by immunohistochemistry with anti-GFAP and anti-vimentin antibodies. *J. Comp. Neurol.* (in press).